



The author(s) shown below used Federal funding provided by the U.S. Department of Justice to prepare the following resource:

Document Title: Nanobiosensor Arrays for On-Site

Multiplexed Detection of Protein Markers to Identify Forensically

Relevant Body Fluids

Author(s): Ashok Mulchandani

Document Number: 310603

Date Received: July 2025

Award Number: 2019-NE-BX-0006

This resource has not been published by the U.S. Department of Justice. This resource is being made publicly available through the Office of Justice Programs' National Criminal Justice Reference Service.

Opinions or points of view expressed are those of the author(s) and do not necessarily reflect the official position or policies of the U.S. Department of Justice.

Federal Award Number: 2019-NE-BX-0006

Project Title: Nanobiosensor Arrays for On-Site Multiplexed Detection of Protein Markers to

Identify Forensically Relevant Body Fluids

Project Director/Principal Investigator (PD/PI):

• Name: Ashok Mulchandani

• Title: Distinguished Professor of Chemical and Environmental Engineering

Contact Information:

Email: <u>adani@engr.ucr.edu</u>

Address: Department of Chemical and Environmental Engineering

900 University Avenue

University of California, Riverside, CA 92521

Tel.: 951-827-6419

Award Recipient Organization:

Regents of the University of California,

University of California, Riverside

Riverside, CA 92521-0217

Project Period: 1/1/2020 – 12/31/2024

Award Amount: \$600,544

Table of Contents

Summary of the Project	.3
Major Goals and Objectives	.4
Research Questions	.4
Research Design, Methods, Analytical and Data Analysis Techniques	.6
1. Aim 1. Develop lateral flow paper-based single-walled carbon nanotube-based chemiresist	or
nanobiosensors for ultrasensitive, selective, and label-free sensing of individual antigen	
biomarkers of blood, semen, saliva, urine and sweat	.6
1.1. Research Design	.7
1.1.1. Sensor Fabrication and Bio-ink Formulation	.7
1.1.2. Signal Acquisition and Testing Protocol	.9
1.2. Results and Findings	
1.2.1. Sensor Appearance and Morphology	10
1.2.2. Bio-Ink Characterization	
1.2.3. Biomarker Sensing Performance	12
2. Aim 2. Develop a fully integrated paper microfluidic single-walled carbon nanotube	es
chemiresistor nanobiosensor arrays for multiplexed sensing of body fluid antigens	15
2.1. Research Design	15
2.2. Results and Findings	15
3. Aim 3. Test and validate the paper microfluidic single-walled carbon nanotubes chemiresist	or
nanobiosensor arrays system for identification of body fluids	
3.1. Research Design	17
3.1.1. Human Sample Testing	17
3.1.2. Species Cross-Reactivity Testing (Animal Fluid Testing)	18
3.2. Results and Findings	18
3.2.1. Testing with Human Blood Samples	
3.2.2. Testing with Human Sweat Samples	21
3.2.3. Testing with Human Saliva Samples	22
3.2.4. Testing with Human Semen Samples	23
3.2.5. Testing with Human Urine Samples	23
3.2.6. Multiplexed Sensing	25
3.2.7. Species Cross-Reactivity Test with Dog Urine and Saliva	26
4. Aim 4. Integrate paper microfluidic chemiresistor nanobiosensor arrays with wireless smart tag	
for facile field sensing	27
4.1, Research Design	27
4.2. Results and Findings	28
Expected Applicability of the Research	31
Limitations	32
Participants and Other Collaborating Organizations	34
Artifacts	
Publications	35
Software and Hardware Artifacts	36
Data Sets Generated	
Dissemination Activities	57

Summary of the Project

The overarching goal of this project was to develop and validate a multiplexed, paper-based chemiresistive biosensor system for the rapid, selective, and on-site identification of multiple body fluids in crime scenes. Existing methods for body fluid identification are often time-consuming, costly, and confined to laboratory settings. This work addresses those limitations by introducing a low-cost, portable sensing platform capable of detecting protein biomarkers associated with blood, semen, saliva, urine, and sweat.

The system is built around a single-walled carbon nanotube (SWNT)-based bio-ink, which integrates the transducer (SWNT) and biorecognition element (antibody) for label-free electrical detection of biomarkers or analytes. The sensor response is recorded as a change in electrical resistance upon target binding (antigen-antibody reaction), allowing quantitative identification in minutes. The project progressed through four structured aims: developing lateral flow paper-based nanobiosensors for individual detection of each body fluid (Aim 1); demonstrating multiplexed detection using purified antigens (Aim 2); validating performance with artificial media and real biological samples (Aim 3); and exploring wireless integration for future field deployment (Aim 4).

The platform demonstrated high sensitivity, specificity, and reproducibility, with minimal cross-reactivity across a range of test conditions. Its paper-based construction and use of water-based inks make it cost-effective, environmental-friendly, and well-suited for point-of-use forensic applications. Overall, the project represents a significant advancement towards accessible, on-site forensic body fluid identification with potential applications in broader point-of-care diagnostics and environmental monitoring.

Major Goals and Objectives:

The **overall goal** of the proposed research was to develop, test and validate a multiplexed sensor device/system for ultrasensitive, quantitative selective, rapid, facile, low cost and on-site identification of multiple body fluids. Towards this goal, specific aims of this project were:

- **Aim 1.** Develop lateral flow paper-based single-walled carbon nanotube-based chemiresistor nanobiosensors for ultrasensitive, sensitive and label-free sensing of individual antigens/biomarkers of blood, semen, saliva, urine and sweat.
- Aim 2. Develop a fully integrated paper microfluidic single-walled carbon nanotubes chemiresistor nanobiosensor arrays for multiplexed sensing of body fluid antigens
- Aim 3. Test and validate the paper microfluidic single-walled carbon nanotubes chemiresistor nanobiosensor arrays system for identification of body fluids
- **Aim 4.** Integrate paper microfluidic chemiresistor nanobiosensor arrays with wireless smart tags for facile field sensing

Research Questions:

Aim 1:

- Can paper-based SWNT sensors reliably detect specific biomarkers from blood, semen, saliva,
 urine, and sweat?
- o Does the sensor exhibit high specificity by producing minimal response to non-target antigens?

Aim 2:

 Can a single integrated paper sensor simultaneously detect multiple body fluid biomarkers from a sample? • What is the cross-reactivity when multiple antibodies are incorporated into a single sensing platform?

Aim 3:

- Can the biosensors detect biomarkers from real human samples recovered from various surfaces and conditions?
- o Is the biosensor able to distinguish human from non-human samples based on species specificity?

Aim 4:

- O How can we design a portable, cost-effective device that maintains accuracy comparable to benchtop systems?
- o How can we detect and mitigate anomalous readings to improve reliability in field settings?
- What hardware and software architecture would best support detachable paper-based sensors
 while enabling wireless communication and continuous data logging?

Research Design, Methods, Analytical and Data Analysis Techniques

1. Aim 1. Develop lateral flow paper-based single-walled carbon nanotube-based chemiresistor nanobiosensors for ultrasensitive, selective, and label-free sensing of individual antigens/ biomarkers of blood, semen, saliva, urine and sweat.

The goal of Aim 1 was to fabricate individual paper-based SWNT chemiresistor biosensors for the label-free detection of purified protein biomarkers associated with five major human body fluids: blood, semen, saliva, urine, and sweat (as listed in Table 1). In addition to these fluid-specific biomarkers, the sensors were also tested with two human-specific proteins: human serum albumin (HSA) and human immunoglobulin G (hIgG). Both HSA and hIgG are abundantly present across multiple body fluids and are unique to human biological matrices, making them valuable for preliminary forensic screening to confirm the human origin of a sample before further analysis.

Protein Biomarker Tested	Body Fluid
Glycophorin A	Blood
Hemoglobin β	Blood
Prostate-specific antigen	Semen
Semenogelin	Semen
Alpha-amylase 1	Saliva
Mucin-5B	Saliva
Osteopontin	Urine
Dermeidin	Sweat

Table 1: Body fluids to be tested and their corresponding biomarkers

This phase of the project established the core sensing framework by combining paper-based microfluidics, printed electronics, and carbon nanomaterial-based biosensing. To enable specific biomarker detection, a bio-ink was developed by functionalizing SWNTs with target-specific antibodies providing the sensing element capable of transducing molecular recognition into an electrical signal. Sensors were tested individually using purified antigens prepared in 10 mM phosphate buffer (PB). Electrical resistance was measured before and after antigen exposure to determine sensor response. This aim successfully demonstrated the platform's sensitivity, specificity, and feasibility for fluid biomarker detection in buffer, validating the bio-ink formulation and fabrication method and establishing the baseline for subsequent multiplexed and real-world testing.

1.1. Research Design

1.1.1. Sensor Fabrication and Bio-ink Formulation

Lateral flow chemiresistor biosensors were fabricated using chromatography paper (Whatman Grade 1) as the substrate. Interdigitated electrodes were patterned on the paper by inkjet printing silver nanoparticle ink (Metalon JS-A191S) using a Fujifilm Dimatix DMP-2831 printer, followed by thermal annealing to form conductive electrical leads. Hydrophobic barriers were then created by wax printing a 5-petal microfluidic channel design on the sensor chip using a Xerox ColorQube 8880DN printer and subsequently melted to allow wax penetration through the paper thickness. An absorption pad was then securely taped on to the sensor to efficiently absorb any excess wash buffer utilized during the data collection steps, in order to maintain consistent humidity levels on the chip's surface to enhance accuracy of the sensor.

To create the transducer, SWNTs were non-covalently modified with 1-pyrenebutanoic acid succinimidyl ester (PBASE), a bifunctional linker enabling π - π stacking onto SWNTs and covalent attachment to antibody primary amines. Initially, SWNTs and PBASE were dispersed in dimethylformamide (DMF) to yield PBASE-functionalized SWNTs. This mixture was vacuum-filtered to remove excess solvent, forming a SWNT/PBASE film, which was then redispersed in 10 mM PB containing Tween-20 and sonicated for uniform dispersion. Subsequently, the target-specific antibody was added and reacted at 4°C for at least 12 hours, forming stable amide bonds with the PBASE succinimidyl esters. This antibody-functionalized dispersion constituted the final bio-ink. Prior to application, the bio-ink was quenched with 0.1 M ethanolamine to deactivate unreacted esters and blocked with 0.05% Triton X-100 to minimize non-specific binding. The workflow is depicted sequentially in Fig. 1. Finally, the bio-ink was drop-casted across the electrode gap on the paper substrate and dried at ambient conditions, completing the functional sensing region of the biosensor.

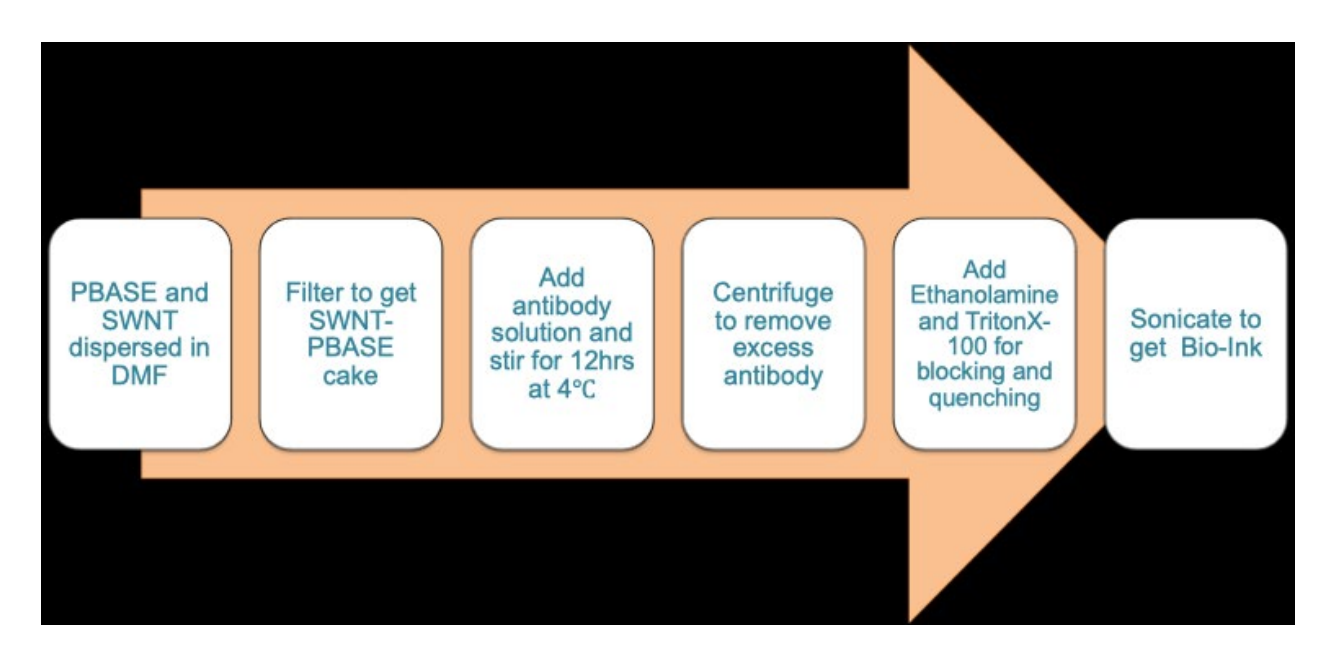


Fig. 1. Bio-ink synthesis protocol

1.1.2. Signal Acquisition and Testing Protocol

Sensor resistance was measured using a Keithley 2450 source meter at a constant voltage of 0.1 V. Baseline resistance was recorded prior to antigen application. Analyte solutions were prepared in 10 mM PB at varying concentrations and applied to the test zone. Following incubation (~15-20 minutes at room temperature), resistances were recorded again to determine the percentage change relative to baseline. Negative controls included sensors with no antibody immobilization (bare SWNT/PBASE) and sensors exposed to non-target antigens. Each test was repeated in duplicate or triplicate (n=10 or 15, n represents number of electrodes) to assess reproducibility.

The sensing mechanism is based on chemiresistive gating, wherein specific antigen binding alters the local electrostatic environment at the SWNT surface. This interaction introduces charge redistribution and steric hindrance, which impede carrier transport within the nanotube network, resulting in an increase in resistance. The magnitude of this resistance changes correlates with antigen concentration, enabling quantitative detection. Fig. 2 provides an overview of the sample testing protocol.

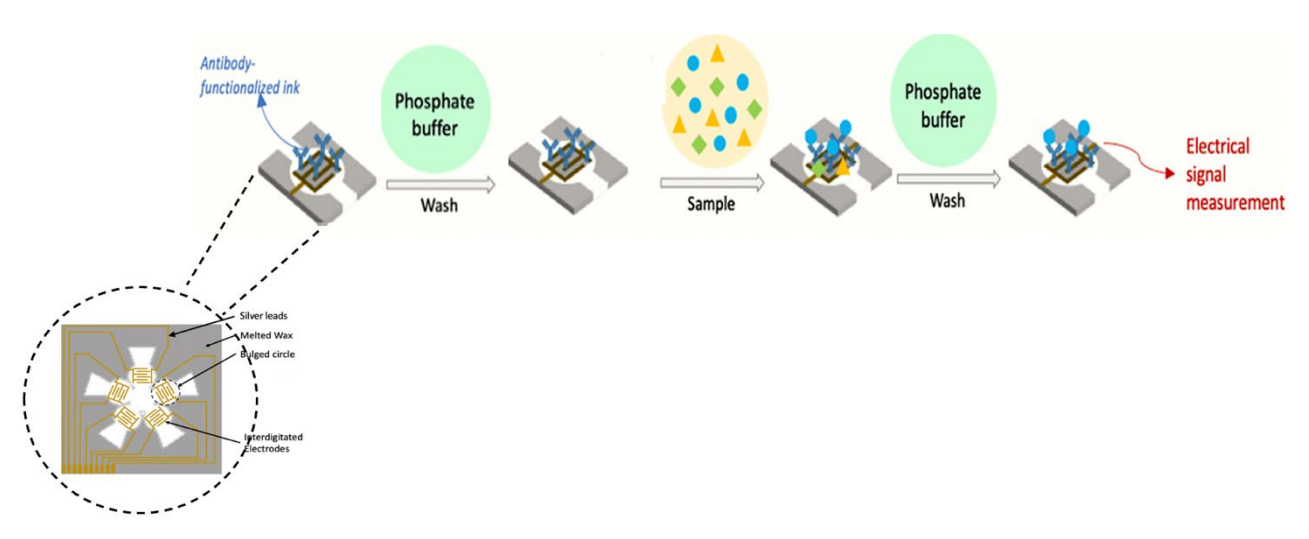


Fig. 2. Overview of testing protocol using Bio-Ink based paper microfluidic nanbiosensor

1.2. Results and Findings

1.2.1. Sensor Appearance and Morphology

The fabricated sensors featured uniform continuous electrical leads and clearly defined wax channels with well-aligned drop-casted SWNT-antibody films bridging the electrode gaps.

1.2.2. Bio-Ink Characterization

To validate successful antibody functionalization of the bio-ink, a series of characterization techniques were performed, which included Fourier-Transform Infrared Spectroscopy (FTIR), Thermogravimetric Analysis (TGA), Raman Spectroscopy, and Ultraviolet-Visible (UV-Vis) Spectrophotometry.

FTIR spectra of individual components (CNT, PBASE, and Anti-HSA Ab) and the final

bio-ink (SWNT/ PBASE/ Anti-HSA Ab) were analyzed to identify characteristic peaks corresponding to functional groups involved the conjugation reaction (Fig. 3). The bio-ink spectrum displayed distinct amide I (~1650 cm⁻¹) and amide II

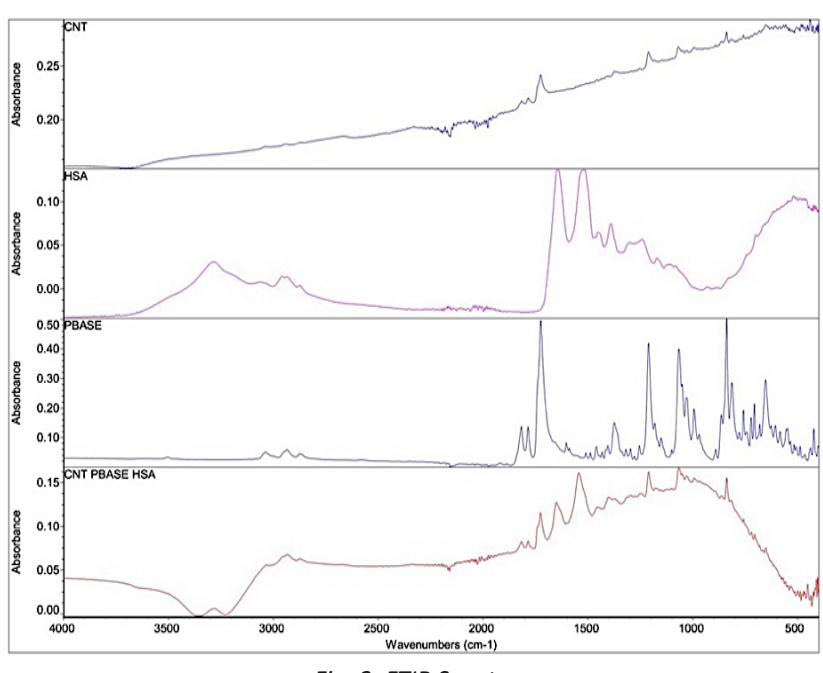


Fig. 3. FTIR Spectra

(~1540 cm⁻¹) peaks, which are associated with the C=O stretching and N-H bending vibrations in the antibody backbone. Additionally, aromatic peaks from PBASE were also retained. The

presence of these features confirmed that the antibodies were successfully immobilized onto the CNTs through PBASE-mediated binding, forming a stable and functional bio-ink suitable for biosensor fabrication.

TGA was performed to further confirm successful antibody functionalization onto the

thermal profiles of CNT/PBASE and CNT/PBASE/Ab (bio-ink) samples were compared to assess mass loss associated with biological molecule decomposition (Fig. 4). The CNT/PBASE/Ab sample exhibited a significantly higher mass loss compared

complex.

The

SWNT/PBASE

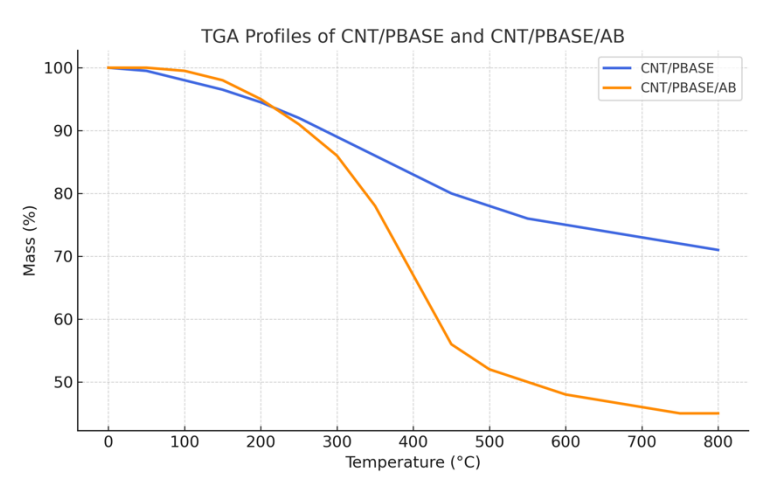


Fig. 4. TGA Curves

to CNT/PBASE, particularly between 200 °C and 500 °C, indicating decomposition of the conjugated antibody. This difference in mass loss, approximately 30–35%, is consistent with thermal degradation patterns of proteins reported in literature, thus validating antibody immobilization on the nanomaterial surface.

Raman plot compared CNT (green), CNT/PBASE (blue), and CNT/PBASE/Anti-HSA antibody or bio-ink (red) samples (Fig. 5). A gradual increase in D-band intensity (~1350 cm⁻¹)

was observed across the samples, indicating successful stepwise functionalization. The consistent G-band (~1580 cm⁻¹) showed that the CNT structure remained intact. These changes confirm effective antibody attachment to the SWNT surface.

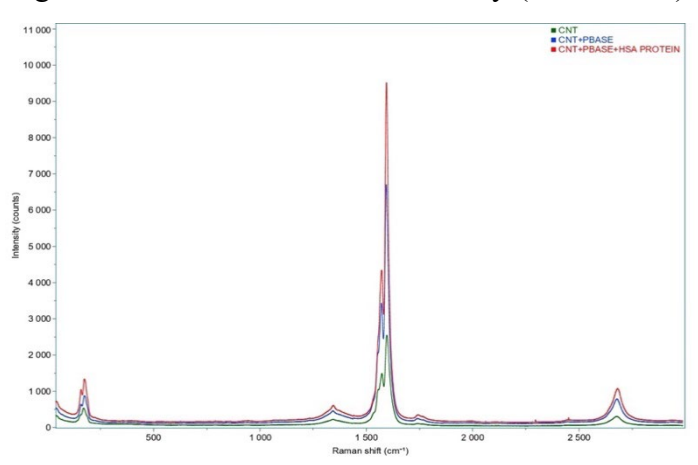


Fig. 5. Raman Spectra

A UV-Vis spectrum analysis (Fig. 6) was also done to confirm antibody conjugation. The absorbance of the supernatant after incubating SWNT/PBASE with antibody solution was compared with that of the original antibody solution. A clear decrease in absorbance at

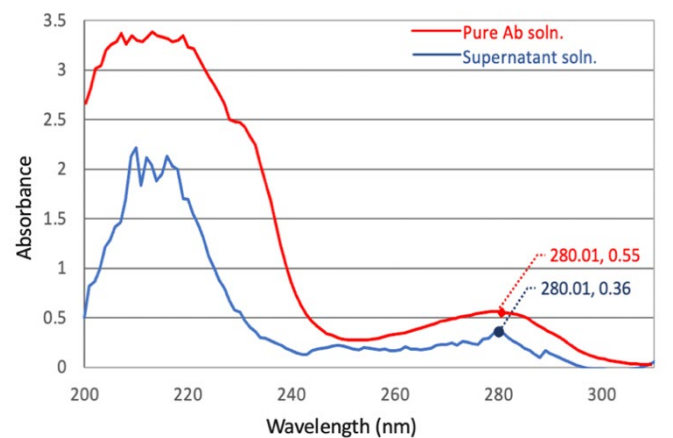


Fig.6. UV-Vis Spectra

280 nm in the supernatant confirmed successful antibody attachment to SWNT/PBASE.

1.2.3. Biomarker Sensing Performance

The fabricated sensors exhibited strong, concentration-dependent increases in resistance upon exposure to their respective target antigens, demonstrating both high sensitivity and specificity. For instance, the sensor functionalized with anti-GYPA bio-ink showed a robust average response of $75.5\% \pm 2.96\%$ when exposed to 1 mg/mL of GYPA, while exhibiting a minimal non-specific response of only $3.53\% \pm 2.17\%$ when exposed to a non-specific 1 mg/mL HSA sample (Fig. 7).

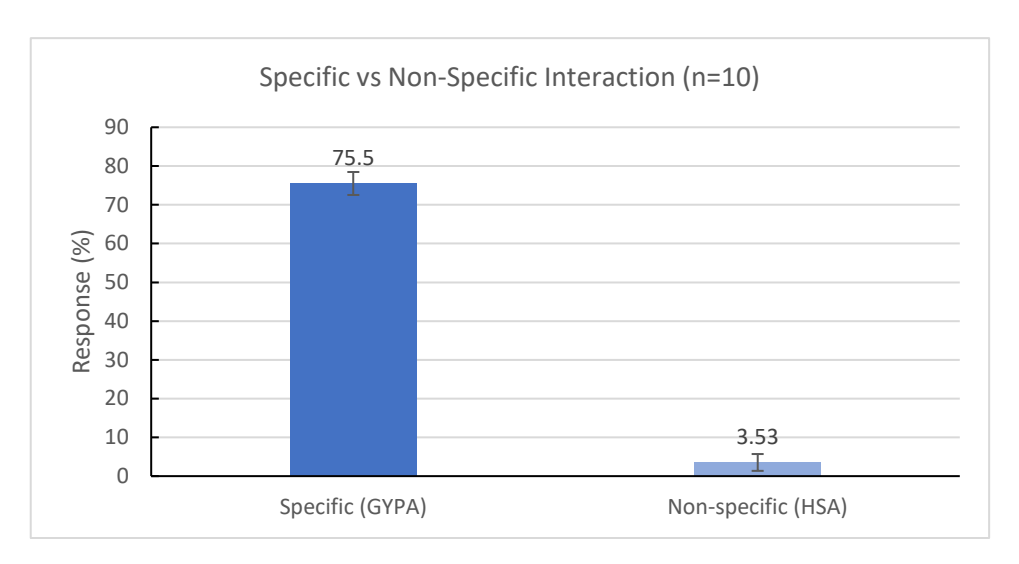


Fig. 7. GPA sensor response

A calibration curve generated for GYPA detection yielded a limit of detection (LOD) of 0.01 mg/mL (Fig. 8).

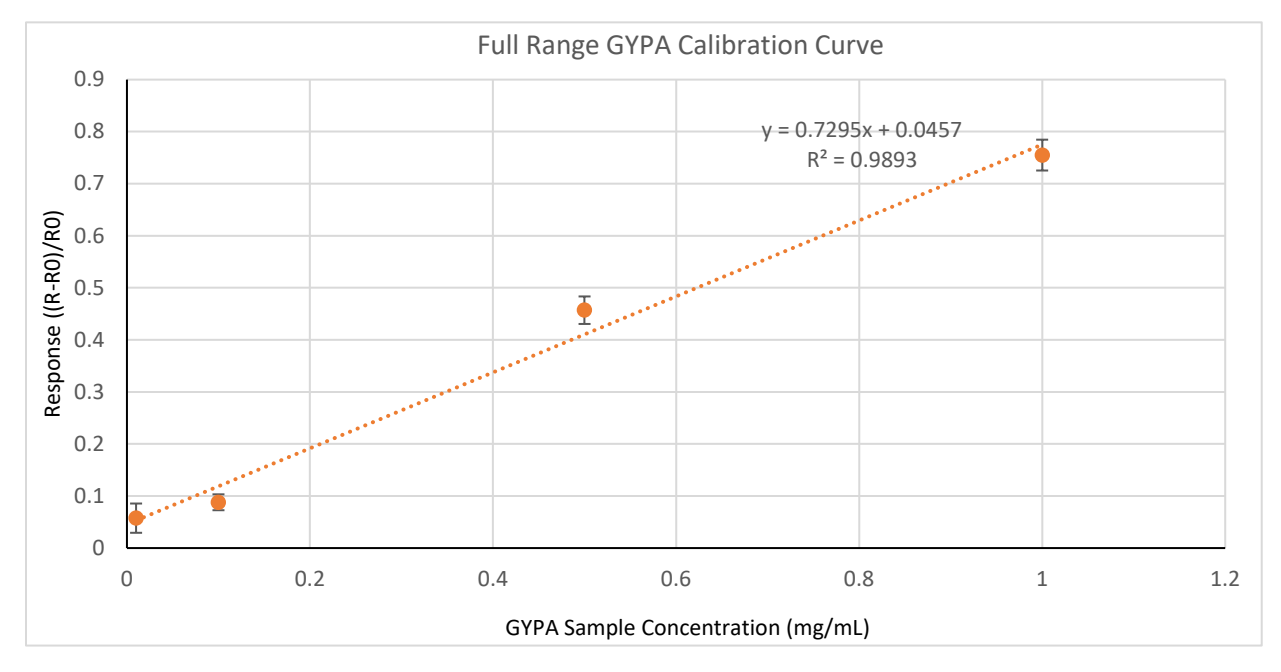


Fig. 8. Full Range GYPA Calibration Curve

Similar analyses were conducted for the other antigen-antibody pairs, with corresponding responses and LODs summarized in the table below (Table 2). All sensors consistently demonstrated high batch-to-batch reproducibility and minimal cross-reactivity. Furthermore,

sensor responses stabilized within 20 minutes of antigen exposure, validating the system's potential for rapid and reliable on-site applications.

Sensor Type / Bio-ink added	Target Biomarker	Conc. Tested (mg/mL)	Specific Response (%)	Non- Specific Response (%)	LOD (mg/mL)	LOQ (mg/mL)
Anti-GYPA	Glycophorin A	1.0	75.5 ± 2.96	3.53 ± 2.17	0.0104	0.0347
Anti-HBB	Hemoglobin β	1.5	85.4 ± 3.13	1.45 ± 1.12	0.0524	0.1747
Anti-SEMG1	Semenogelin-1	0.5	47.15 ± 5.52	2.26 ± 1.85	0.0156	0.0519
Anti-PSA*	Prostate-specific antigen		55.98 ± 4.07	6.05+/- 2.13		
Anti-AMY1	Alpha-amylase 1	0.26	17.87 ± 2.12	2.87 ± 1.1	0.028	0.093
Anti- MUC5B	Mucin-5B	1.5	74.1 ± 3.44	3.17± 1.17	0.129	0.391
Anti-HSA	Human Serum Albumin	2.0	80.97 ± 3.09	4.75 ± 3.97	0.1011	0.3061
Anti-hIgG	Human Immuno- globulin G	2.0	71.72	4.53	0.07	0.212
Anti-OPN	Osteopontin	0.1	10.78 ± 1.68	1.51 ± 1.04	0.0102	0.03147
Anti-DCD	Dermcidin-1	0.05	91.98 ± 3.41	2.24 ± 5.31	0.001	0.003

Table 2. Summary of sensor responses

* We were unable to determine the exact concentration of the sample used, and thus could not generate a reliable calibration curve. According to the Sigma-Aldrich specification sheet, the stock concentration of the compound ranged between 1.0 and 5.0 mg/mL. As a result, our diluted sample could have had a concentration anywhere between 0.06 mg/mL and 0.3 mg/mL.

2. Aim 2. Develop a fully integrated paper microfluidic single-walled carbon nanotubes chemiresistor nanobiosensor arrays for multiplexed sensing of body fluid antigens

The goal of Aim 2 was to demonstrate the multiplexing capability of the paper-based SWNT chemiresistive biosensor system by simultaneously testing a single sample for the presence of multiple body fluid biomarkers. This marked a critical transition from single analyte detection (Aim 1) to a fully integrated, multiplexed format optimized for forensic applications where sample volume may be limited.

2.1. Research Design

To implement multiplexed detection, each type of SWNT-antibody ink was deposited into a dedicated channel, creating spatially separated but electrically independent sensing zones. Purified antigens diluted in 10 mM PB were applied centrally (15-20ul in volume) to each sensor such that the sample passed through all five channels simultaneously and resistance changes were recorded for each channel.

2.2. Results and Findings

The multiplexed paper-based SWNT chemiresistive biosensor system successfully demonstrated the ability to detect the presence of multiple body fluid biomarkers simultaneously from a single sample. Fig. 12 gives a summary of the sensor responses for different multiplexed tests.

In the SEMG-1 test, the platform featured five distinct antibody-functionalized channels: Anti-GYPA, Anti-SEMG, Anti-OPN, Anti-MUC5B, and Anti-DCD (Fig. 9). 0.3 mg/mL SEMG-

1 sample was applied centrally. Only the Anti-SEMG1 channel exhibited a strong specific response of 34.25%, while other channels remained low, averaging $0.88\% \pm 1.91\%$.

In the HBB multiplexed test, channels were functionalized with Anti-HBB, Anti-PSA, Anti-hIgG, and Anti-HSA bio-inks and a control (no antibody) (Fig. 10). A 1 mg/mL HBB sample was used. The Anti-HBB channel produced a strong specific response of 74.84%, while non-specific channels averaged 7.01%, and the control channel recorded $2.1\% \pm 1.79\%$.

For detecting HSA in sample, the multiplexed sensor included three Anti-HSA channels, along with Anti-HBB and Anti-PSA (Fig. 11). A 1.5 mg/mL HSA sample was added centrally. The Anti-HSA channels produced consistent responses averaging $73.02\% \pm 2.5\%$, while the non-specific average was $5.79\% \pm 1.5\%$.

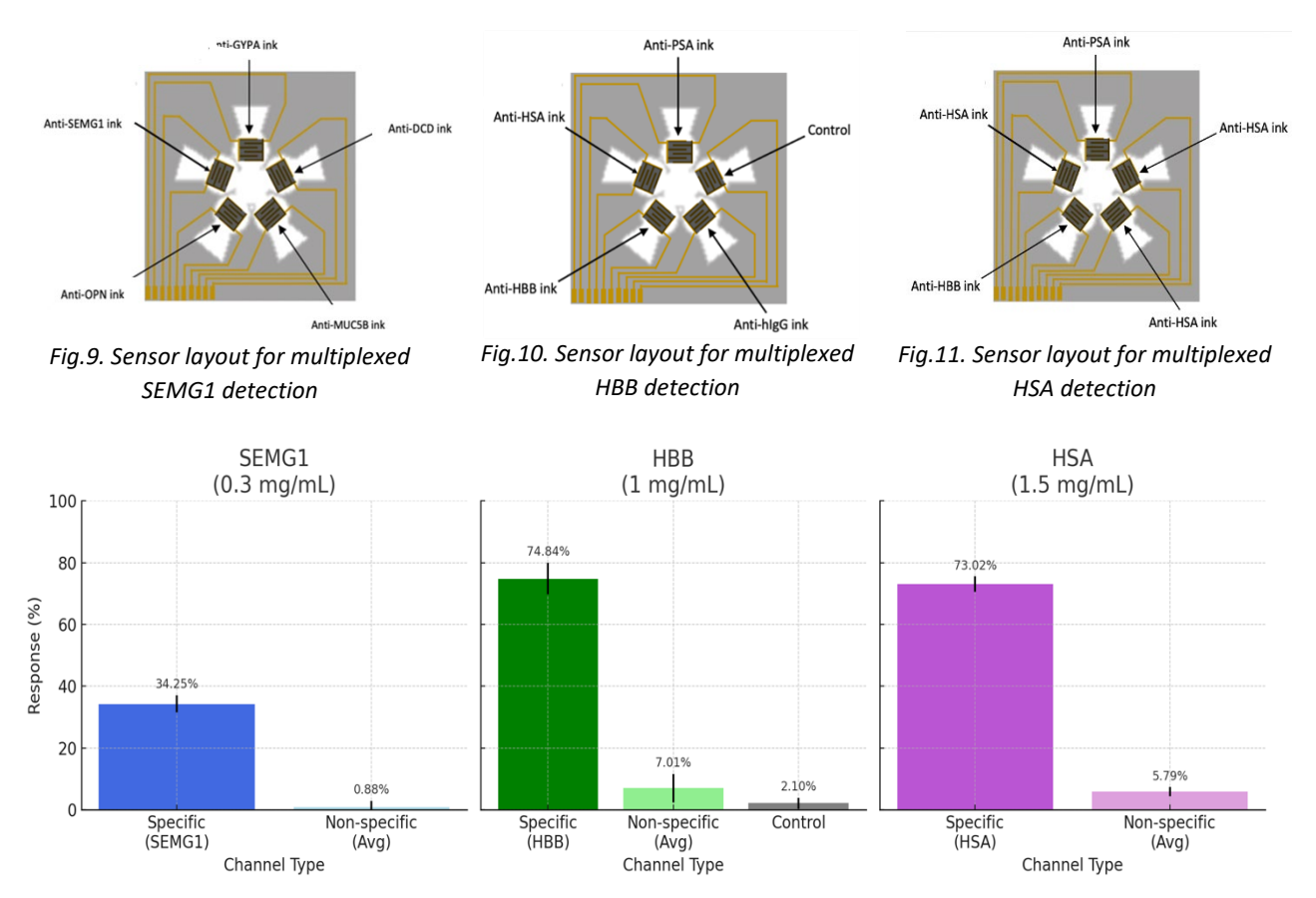


Fig. 12. Normalized sensor responses for multiplexed tests using purified protein antigens of SEMG1, HBB, and HSA, respectively

3. Aim 3. Test and validate the paper microfluidic single-walled carbon nanotubes chemiresistor nanobiosensor arrays system for identification of body fluids

The objective of Aim 3 was to evaluate the performance of the biosensor system in realistic sample conditions, extending beyond buffer-based purified antigen testing. This phase focused on assessing the sensor's sensitivity, specificity, and reproducibility when exposed to complex matrices, including both artificial body fluid simulants and real human biological samples. Multiplexed sensing was also tested using real samples to assess the system's ability to discriminate multiple body fluids simultaneously within a single platform. Additionally, this aim explored the impact of practical sample collection methods as well as retrieval of samples from different surfaces to simulate forensic evidence handling at crime scenes. By validating the sensor under these conditions, this aim bridges the gap between laboratory feasibility and field applicability, establishing the robustness of the system for potential on-site forensic screening.

3.1. Research Design

3.1.1. Human Sample Testing

To mimic forensic field conditions, human body fluid samples (blood, saliva, semen, urine and sweat) were deposited on various surfaces, including glass, cloth, metal, and synthetic polymer. Sensors were tested after retrieval using two main collection methods:

a. *Swabbing*: Cotton swabs moistened with 10 mM PB were used to collect dried stains, which were then reconstituted in buffer for testing.

b. *Direct extraction*: For stained fabrics, portions were submerged and squeezed in buffer to extract the analyte.

Blood samples required additional lysis step after retrieval using hemolysis buffer before addition to sensors. Multiplexed sensing was also performed to demonstrate simultaneous detection capability of sensors and confirm channel independence.

3.1.2. Species Cross-Reactivity Testing (Animal Fluid Testing):

To assess specificity across species, sensors containing Anti-HSA and Anti-hIgG bio-inks quenched and blocked with 0.1 M ethanolamine and 40mM PEG400 respectively were tested against dog saliva and dog urine. The samples were applied to center of the sensors and allowed to incubate for approximately 15-20 minutes at room temperature. Resistance measurements were taken before and after exposure to determine the normalized response for each antibody channel.

3.2. Results and Findings

3.2.1. Testing with Human Blood Samples

To assess blood detection using the biosensor platform, experiments were conducted with sensors functionalized using Anti-GYPA and Anti-HBB bio-inks. For the Anti-GYPA sensors, 10 µL of whole human blood was deposited onto glass slides and allowed to dry at room temperature for up to 14 days. Dried blood residues were collected using moistened cotton swabs and reconstituted in 1X lysis buffer before sensor application. To simulate various crime scene environment conditions, additional blood stains were stored for up to 14 days under: cold conditions (4 °C) to mimic refrigerated storage or cold climate, and elevated temperatures (40 °C) to simulate exposure to heat

or summer outdoor scenes. In each case, samples were retrieved using the same swabbing and reconstitution method. The reconstituted samples were applied to Anti-GYPA functionalized sensors, and the responses were recorded. The biosensor platform demonstrated robust and consistent responses for samples stored at room temperature and 4 °C, even up to 14 days post-deposition. However, samples stored at 40 °C exhibited a progressive decline in response, implying that continuous elevated heat may cause degradation or denaturation of the target biomarkers. These results highlight the sensor's suitability for forensic body fluid analysis, especially in time-delayed evidence retrieval scenarios. The platform maintains detection reliability under typical conditions, with only extreme heat impacting sensitivity. Fig. 13 shows a comparison of the sensor responses.

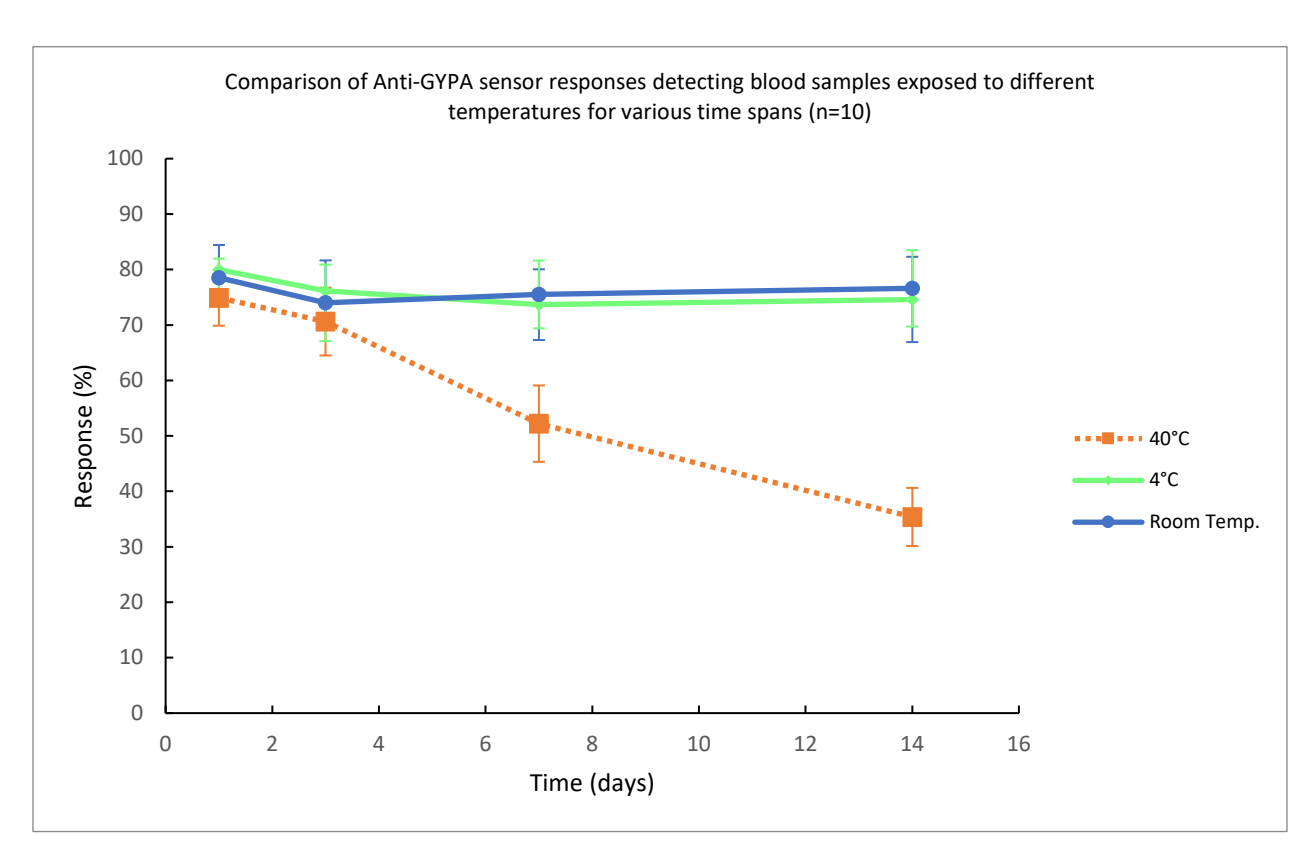


Fig. 13. Comparison of Anti-GYPA sensor responses detecting blood samples exposed to different temperature for various time spans

For testing with Anti-HBB sensors, first 200 µL of whole human blood was deposited onto both glass slides and cloth pieces and allowed to dry at room temperature for 24 hours. Glass samples were retrieved by swabbing the surface and reconstituting the swab in 1X lysis buffer, and cloth samples were retrieved by both swabbing and by directly cutting a piece of the stained cloth and submerging it in buffer. Both methods resulted in significant sensor responses, confirming effective recovery of the target analyte. Notably, direct extraction from cloth yielded higher signal intensity than swabbing of cloth, likely due to more efficient release of the biomarker. A control sensor lacking antibody showed minimal response, validating the specificity of the detection. Fig. 14 gives a side-by-side comparison of all the responses.

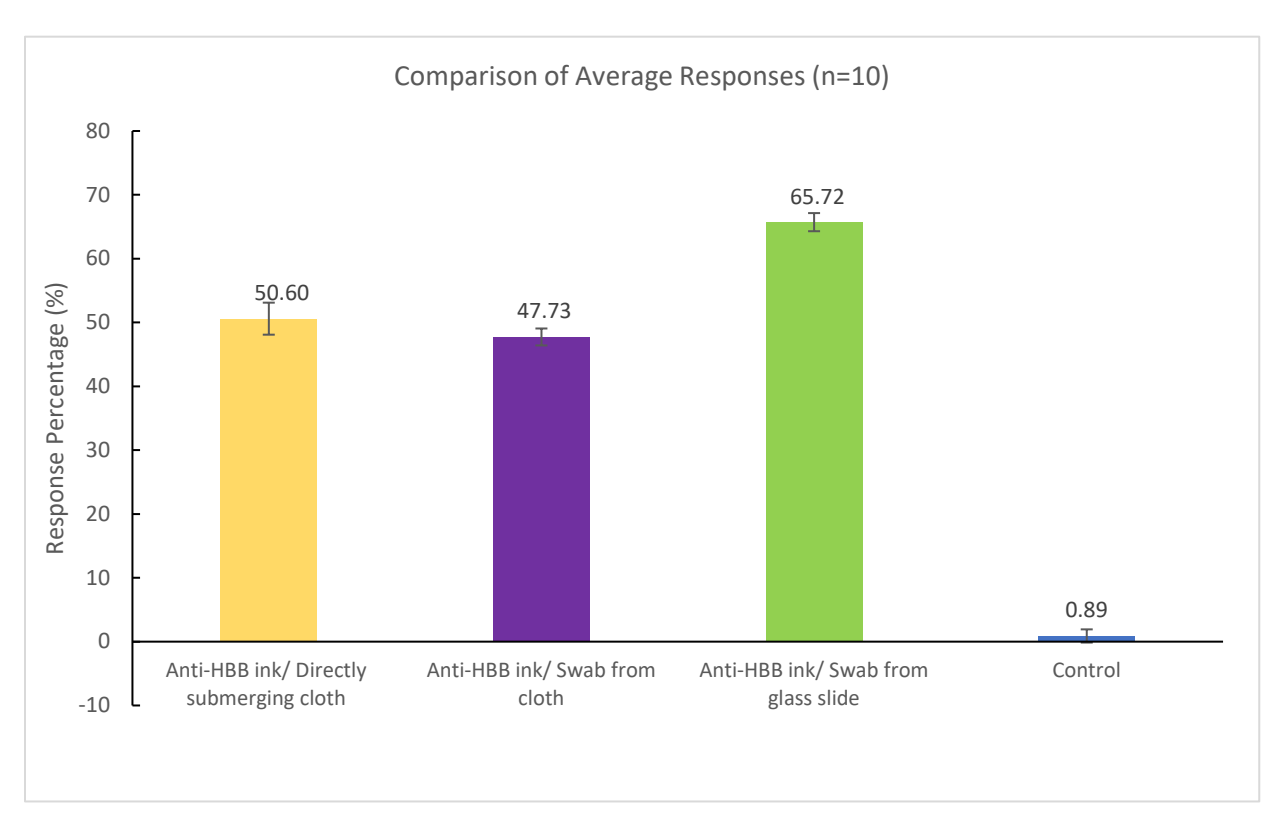


Fig. 14. Comparison of Anti-HBB sensor responses

To simulate environmental stress, blood-stained glass slides were also stored for up to 14 days at 4 °C and 40 °C. Consistent and robust responses were obtained from cold-stored samples, while samples stored at elevated temperatures showed decreased but still considerable responses,

reaffirming the platform's applicability in temperature-stressed forensic recovery scenarios (Fig. 15).

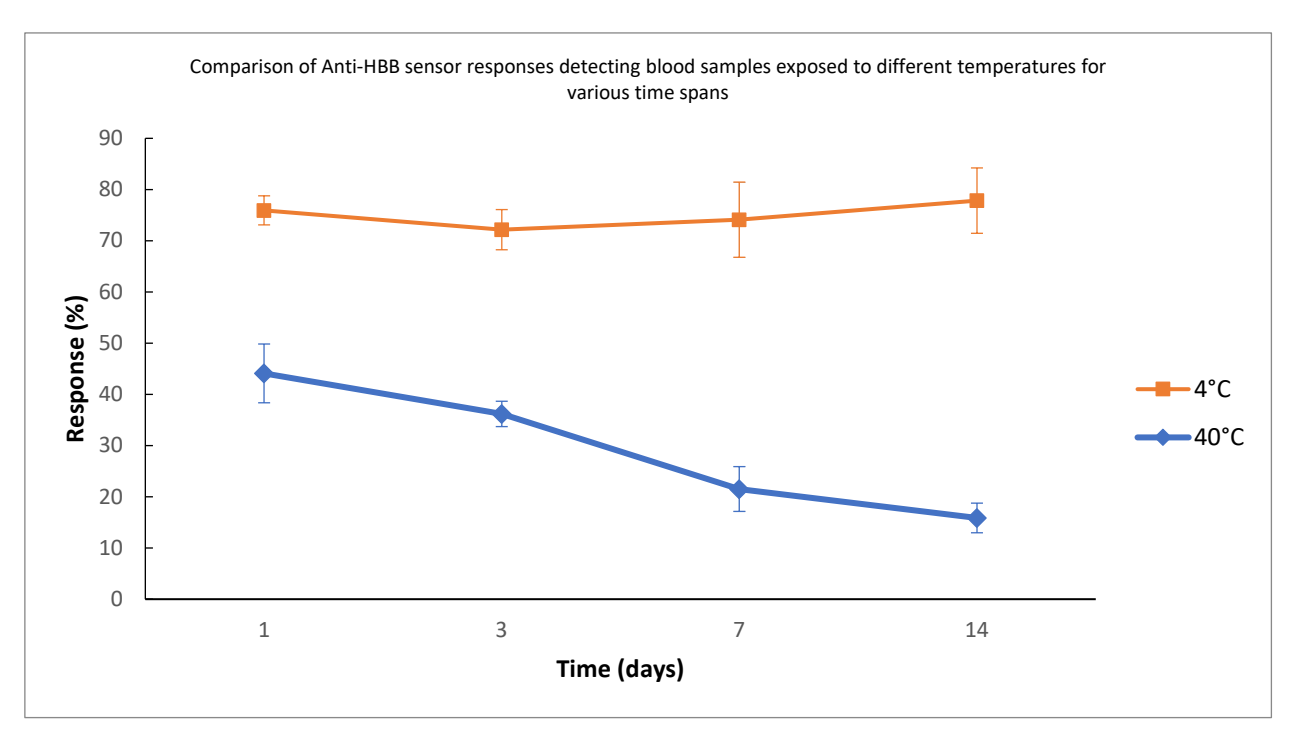


Fig.15. Comparison of Anti-HBB ink sensor responses detecting blood samples exposed to 4°C and 40°C for various time spans

3.2.2. Testing with Human Sweat Samples

A 20 µL sweat sample was deposited on a nitrile glove surface and allowed to dry for 3 hours at room temperature to simulate trace-level forensic evidence. The dried sample was recovered using a moistened cotton swab and reconstituted in

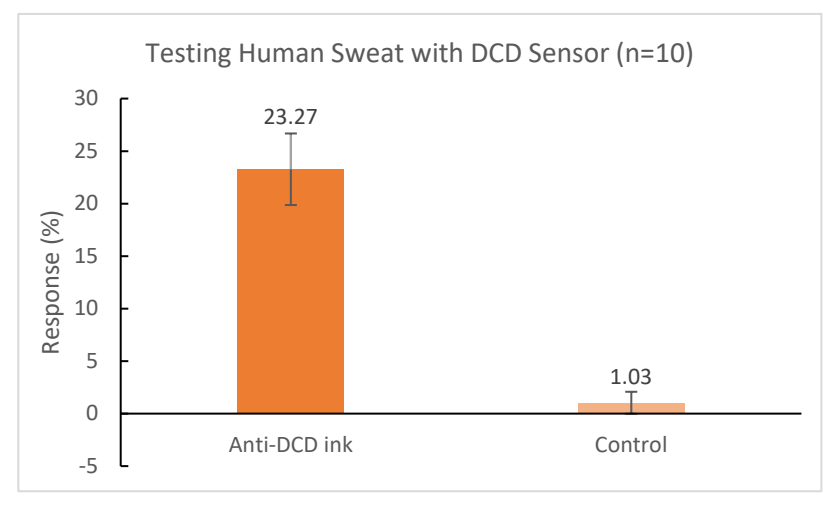


Fig.16. Comparison of Anti-DCD ink sensor responses: specific vs control

400 μ L of PB. The sample was then tested using a sensor with Anti-DCD bio-ink. A strong response of 23.27% \pm 3.4% was observed and a control test was also performed which gave a response of 1.03% \pm 1.04% (Fig. 16). Based on the calibration curve and accounting for the 21-fold dilution, the concentration of DCD in the original sample was calculated to be approximately 26.6 μ g/mL. This value falls within the reported physiological range for DCD in human sweat, providing further validation of the sensor's sensitivity and real-sample applicability.

3.2.3. Testing with Human Saliva Samples

Saliva samples were collected using two different approaches. In the first, residue was recovered from the rims of used aluminum can using a moistened cotton swab, reconstituted in 1 mL PB, and applied to sensors functionalized with anti-AMY1 bio-ink. This setup yielded a strong specific response of $24.32\% \pm 4.72\%$, while the control showed a minimal signal of $1.11\% \pm 2.19\%$, confirming selectivity (Fig. 17).

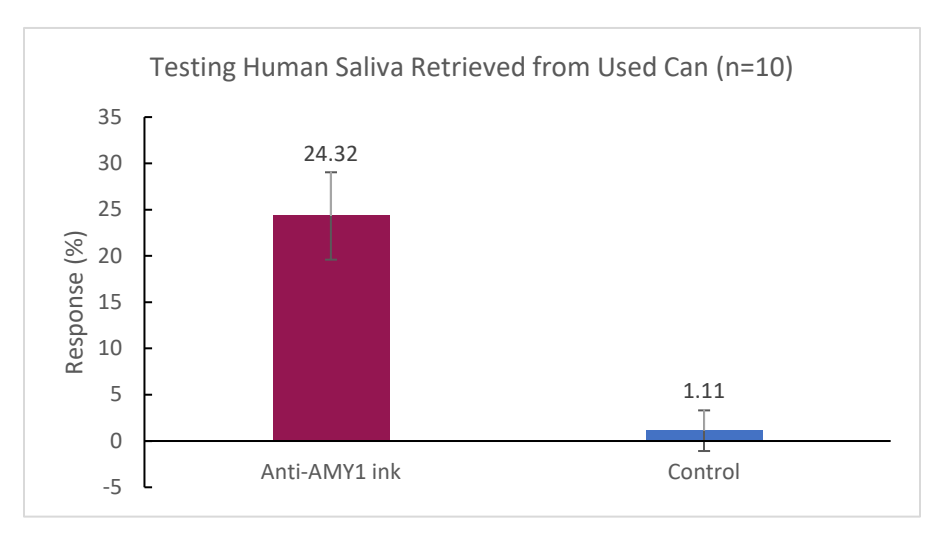


Fig.17. Comparison of Anti-AMY1 ink sensor responses: specific vs control

In the second approach, 25 μ L of saliva was deposited onto a glass slide, air-dried at room temperature, then swabbed and reconstituted in 200 μ L buffer (8-fold dilution). The resulting sample produced a sensor response of 32.49% \pm 2.19%. Using the calibration curve, the

concentration of alpha-amylase in the undiluted sample was calculated to be approximately 3.47 mg/mL, which lies within the physiological range. These findings further affirm the biosensor's sensitivity and its effectiveness in real-world forensic or diagnostic applications.

3.2.4. Testing with Human Semen Samples

10 μL of human semen was spotted on a glass slide and allowed to dry at room temperature.

Sample was collected using moistened cotton swab and reconstituted in PB, resulting in a 100fold dilution. The reconstituted sample tested using was sensor functionalized with Anti-SEMG1 bioink which produced a strong response of $16.07 \pm 2.22\%$. Using the SEMG1 calibration curve, and factoring in the

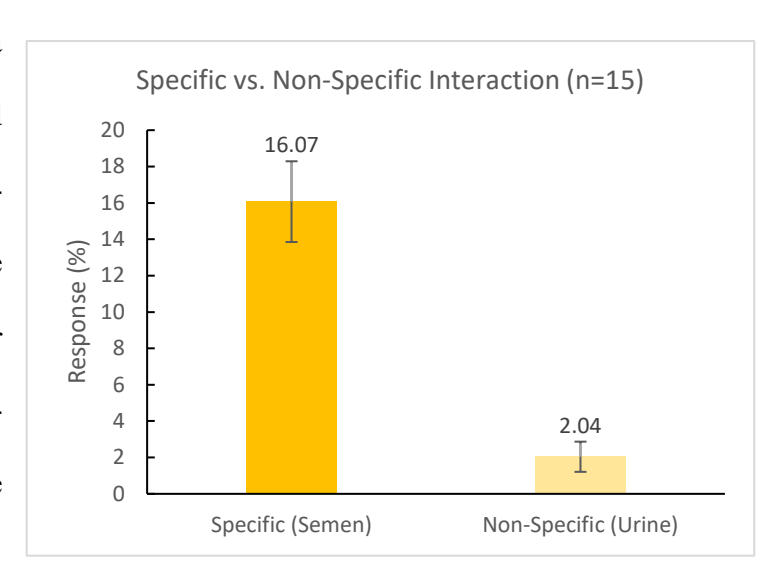


Fig.18. Comparison of Anti-SEMG1 ink sensor responses: specific vs non-specific

dilution, the original SEMG1 concentration in semen was estimated to be \sim 8.12 mg/mL, which is consistent with the physiological range reported in literature. A non-specific response of $2.04 \pm 0.83\%$ was observed when a urine sample was also tested on another sensor, further supporting the sensor's specificity. This validates the sensor's accuracy and applicability in forensic body fluid identification. Fig. 18 gives a side-by-side comparison of the sensor responses.

3.2.5. Testing with Human Urine Samples

50 μL of human urine was spotted on a glass slide and allowed to dry at room temperature. Sample was collected using a moistened cotton swab and reconstituted in PB, resulting in a 2-fold dilution.

The reconstituted sample was tested using a sensor functionalized with Anti-OPN bio-ink which produced a response of $1.49\% \pm 0.88\%$. A control was also tested which gave a response of $0.59\% \pm 0.38\%$ (Fig. 19).

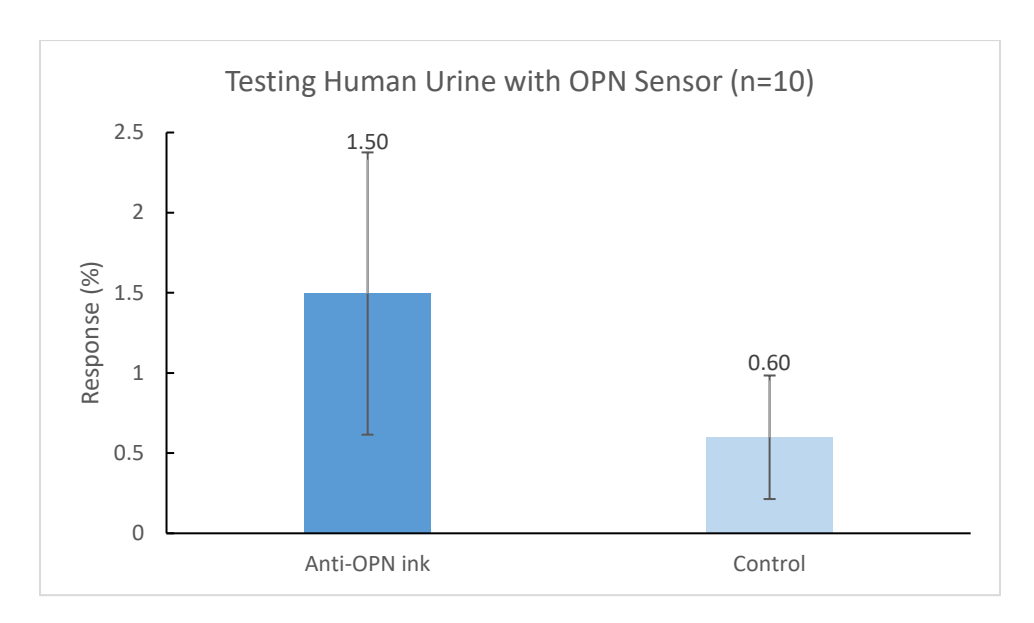


Fig.19. Comparison of Anti-OPN ink sensor responses: specific vs control

This low signal indicates that 50 μ L of human urine may not contain sufficient OPN for detection within the sensor's response range, especially after dilution. It is important to note that OPN concentration in urine can vary significantly depending on the time of day, hydration level, and individual biological variability, all of which influence both the total volume and protein content of urine.

So, in order to validate the performance and sensitivity of the biosensor, an artificial urine medium (AUM) was prepared and spiked with known concentrations of OPN. This controlled approach eliminated variability and allowed precise evaluation of the sensor's ability to detect OPN in a urine-like environment. Results from these tests are discussed in the following section.

Artificial Urine Medium (AUM)

Artificial Urine Medium (AUM) was prepared following an established protocol obtained from

literature and spiked with 0.3 mg/mL OPN. The sample was tested directly on the anti-OPN sensor, and it produced a strong average response of $20.45\% \pm 4.76\%$, confirming its sensitivity in complex urine-like media. As a negative control, AUM with no OPN was tested similarly and a

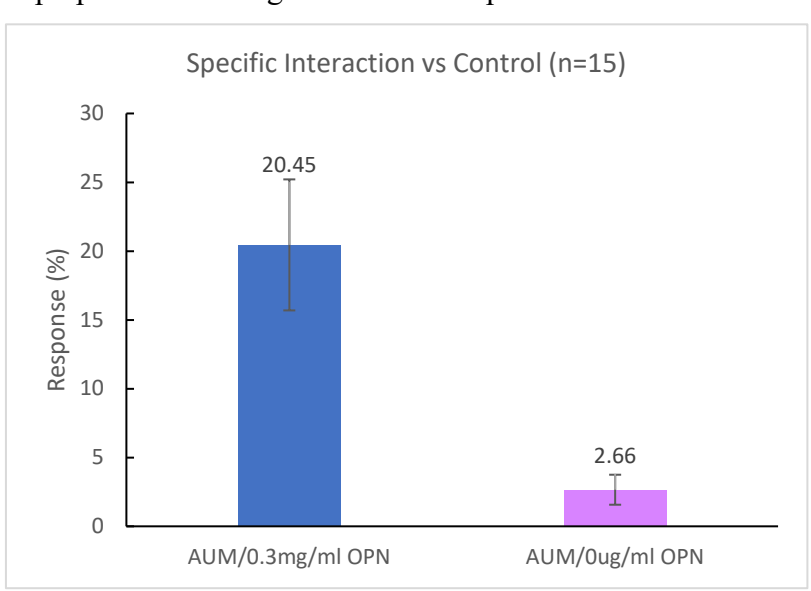


Fig.20. Comparison of Anti-OPN ink sensor responses with AUM: specific vs control

very low response of only 2.66% \pm 1.09% was recorded. (Fig. 20). Next, to mimic dried trace evidence, 20 μ L of AUM spiked with 0.3mg/mL OPN was deposited on a glass slide and dried for 10 hours at 25 °C. The dried residue was swabbed using a moistened cotton swab and reconstituted in 100 μ L of 10 mM phosphate buffer prior to testing. The sensor generated a substantial response of 8.59% \pm 3.04%, aligning well with the calibration curve and direct testing results, thereby validating surface recovery efficiency.

3.2.6. Multiplexed Sensing

To confirm the multiplexed sensing capability of the biosensor using real human samples and to further validate its specificity with minimal cross-reactivity, a sensor was fabricated with five different antibody-functionalized bio-inks: anti-HBB, anti-GYPA, anti-DCD, anti-OPN, and anti-SEMG1. When a diluted human blood sample was applied, the anti-HBB and anti-GYPA channels displayed strong responses of 79.49% and 82.55%, respectively. In contrast, the remaining non-

targeted channels (anti-DCD, anti-OPN, anti-SEMG1) showed minimal average responses of

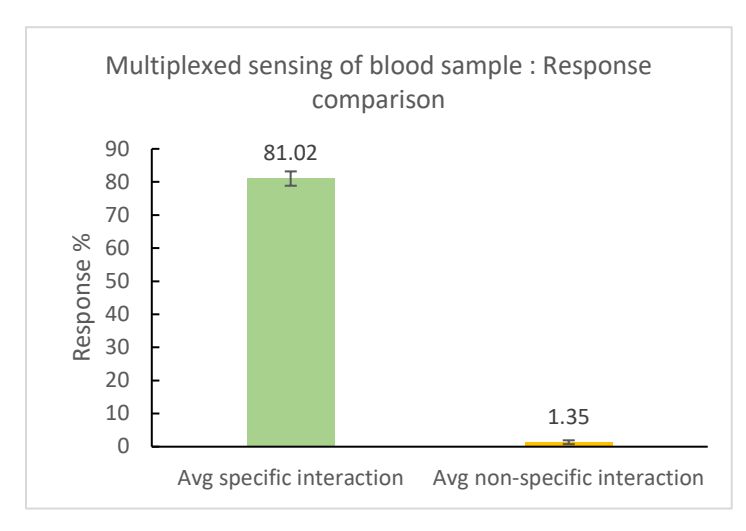


Fig.21. Multiplexed sensing of blood sample

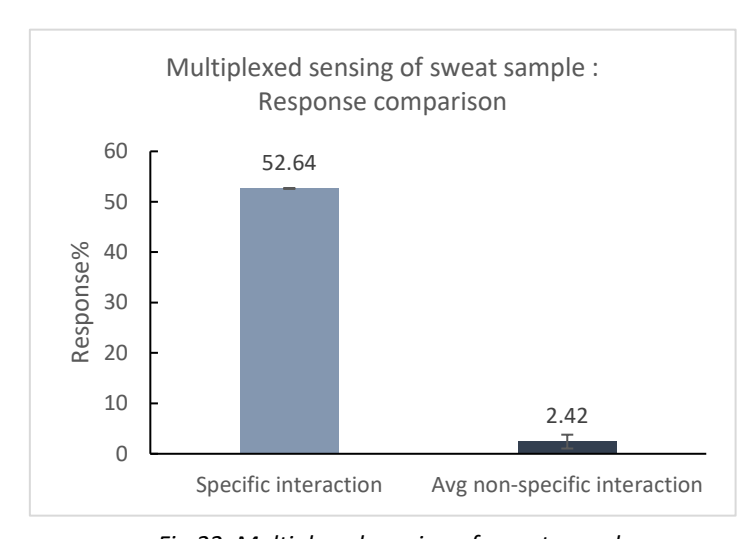


Fig.22. Multiplexed sensing of sweat sample

 $1.34\% \pm 0.58\%$, confirming high sensor specificity (Fig. 21).

Similarly, when a diluted human sweat sample was tested on a sensor containing anti-HBB, anti-MUC5B, anti-DCD, anti-OPN, and anti-SEMG1 bio-inks, only the anti-DCD channel responded strongly (52.64%), while the others averaged a low response of 2.42% ± 1.37% (Fig. 22). These findings highlight the platform's ability to selectively detect target biomarkers in complex sample matrices, making it highly suitable for forensic applications.

3.2.7. Species Cross-Reactivity Test with Dog Urine and Saliva

When exposed to dog urine, the Anti-hIgG sensor exhibited a minimal normalized response of $2.13\% \pm 1.94\%$, while the Anti-HSA sensor showed an even lower signal of $1.29\% \pm 1.4\%$. Next the biosensor system was tested with dog saliva using sensors with Anti-HSA and Anti-hIgG bio-inks. The responses were consistently low, with Anti-HSA showing a normalized response of $1.46\% \pm 0.89\%$ and Anti-hIgG showing $1.52\% \pm 0.55\%$. These low responses, significantly below

responses observed for human samples, demonstrate the sensor's high specificity for human proteins, minimizing the likelihood of false positives from animal-origin contamination in real-world forensic scenarios. Fig.23 gives a response comparison of the two sensors.

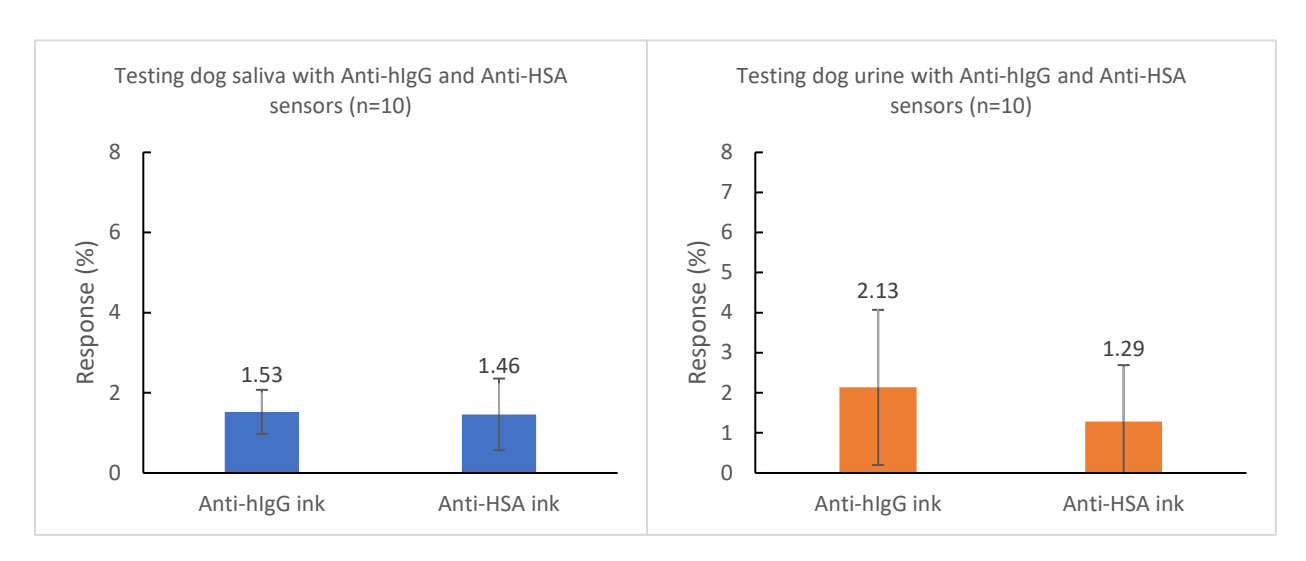


Fig.23. Responses to dog urine and saliva: Anti-hlgG and Anti-HSA sensors

4. Aim 4: Integrate paper microfluidic chemiresistor nanobiosensor arrays with wireless smart tags for facile field sensing

This phase focused on developing and validating a portable smart tag system (Halibut) capable of wireless impedance measurement for field-deployable biosensing.

4.1. Research Design:

A systematic design approach was employed that integrated hardware development, firmware implementation, and machine learning techniques. A custom 6-layer printed circuit board (PCB) was designed with careful attention to signal integrity, achieved through optimized routing,

shielding, and component placement. The hardware architecture included communication modules (USB, Bluetooth Low Energy 5.2), an ARM Cortex-M3 microcontroller, and a multichannel analog front-end for sensor interfacing.

For data acquisition and analysis, Electrochemical Impedance Spectroscopy (EIS) was implemented at 100 Hz with a 40 mV signal to measure impedance, offering faster readings than traditional embedded potentiostat designs and avoiding charging current issues. The acquired raw impedance data underwent normalization and preprocessing prior to analysis.

For anomaly detection, a semi-supervised deep learning approach was adopted, using a Bidirectional Gated Recurrent Unit (BiGRU) autoencoder model. This model was chosen for its efficiency in handling sequential data without requiring explicit feature engineering. The model was trained on normal sensor behavior data and used reconstruction error to identify anomalies. A dynamic thresholding technique using Gaussian filtering was implemented to adapt to varying sensor behaviors while maintaining detection sensitivity.

Validation of the system was performed through: (i) a side-by-side comparison with Keithley benchtop instruments using standardized passive components, (ii) correlation analysis with actual paper-based sensors using deionized water and phosphate buffer samples, and (iii) performance testing of the anomaly detection algorithm against artificially induced anomalies of varying severities.

4.2. Results and Findings:

A complete prototype smart tag hardware system, named Halibut (Fig. 24) was developed, featuring a custom 6-layer printed circuit board with 5-channel sensor interface, an analog front

end with integrated 16-bit ADC for precise measurements, an ARM Cortex-M3 processor with

+5V

Response

BLE for wireless communication, USB connectivity for data transfer and power, and temperature and humidity sensors for environmental monitoring.

Firmware and software systems were created, including C/C++ firmware for microcontroller operation and sensor interfacing, Kivy-based crossplatform GUI for data visualization, and device control and data logging on both PC and Android

LDO

Fig.24. Halibut Block Diagram and Prototype

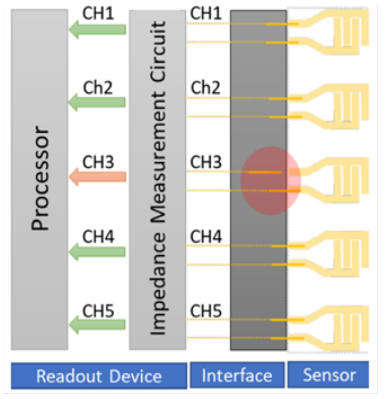
devices (Fig. 25).

Correlation studies between the Halibut platform Keithley and benchtop equipment validated

No Anomaly	Low	Continue	
No Allomary	Low	Measurements	
Sample		Continue	
	Low	Measurements,	
Placement	Low	System working	
		as intended	
		Faulty or Bad	
Connection	Moderate	Connection,	
		Inspect Interface,	
		Reconnect, or get	
		a new sensor	
		Continue	
Glitch	Moderate	Measurements,	
		Ignore erroneous	
		data	
No Sensor	High	Get new sensor	
Procedural	High	Get new sensor	

Anomaly Source





(b) Example: "Bad Connection" anomaly in CH3

error rates of only 0.4-0.6% in

measurement accuracy with

measurements of standard resistive components and actual sensor samples (Fig. 26), while demonstrating significantly faster measurement capability (8 seconds vs. 30+ seconds per reading), which validates its suitability for field applications requiring laboratory-grade



Fig.25. Type of Anomalous Behaviors and Example

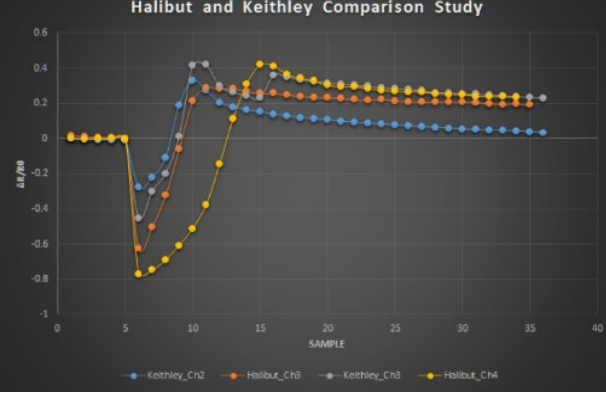


Fig.26. Comparison of Halibut and Keithley Measurements

precision. Sensor scheduling strategies were also investigated to enable resource-efficient event classification.

The hardware design also achieved substantial improvements over other comparable mobile measurement systems, specifically lower component count (22 parts vs. 48–70 parts in prior systems), reduced cost (~\$25 vs. \$60+), faster response time (~8 seconds per reading vs. 30+ seconds), and multimodal communication (wired and wireless vs. wireless only). The EIS measurement approach provided faster readings than traditional DC methods while maintaining accuracy, avoiding charging current issues that require additional settling time.

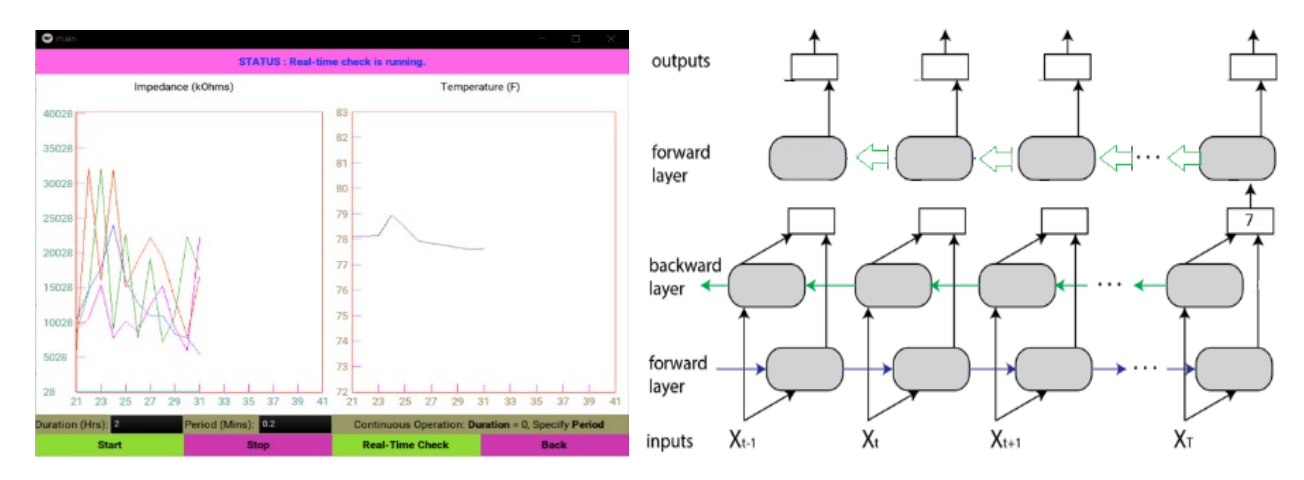


Fig.27. Halibut cross-platform GUI software

Fig.28. BiGRU-based autoencoder model

Various types of anomalies were classified based on severity levels: (i) low (e.g., normal sample placement events), (ii) moderate (e.g., connection issues and signal glitches), and (iii) high (e.g., missing sensors and procedural errors) (Fig. 27). The anomaly detection system was implemented and validated using Bidirectional Gated Recurrent Unit (BiGRU) autoencoder neural networks (Fig. 28). Models were developed to effectively identify anomalous sensor behavior, and dynamic thresholding techniques were incorporated to adapt to varying conditions.

Our Hal-BG anomaly detection model achieved a detection accuracy of 98.3%, precision of 85.8%, and recall of 79.6% across various test scenarios, significantly outperforming conventional approaches like the naïve threshold method (95.5% accuracy, but only 25% precision) and ARIMA (71.8% accuracy) (Table 3).

Testing with various sample applications demonstrated that our system can reliably detect changes in impedance when biological fluids are applied to paper-based sensors, with consistent behavior across multiple sensors, confirming both sensitivity and practical reliability of the smart tag platform.

Metrics	HAL-BG	Naïve Threshold	ARIMA
Accuracy	98.3%	95.5%	71.8%
Precision	85.8%	25.0%	77.5%
Recall	79.6%	85.7%	71.6%
F _{Score}	0.82	0.33	0.13

Table 3: Comparison of Hal-BG against other methods

Expected Applicability of the Research

The biosensor platform developed in this research holds strong potential to transform forensic investigations by enabling rapid, label-free, on-site identification of human body fluids (specifically blood, semen, saliva, urine, and sweat) at crime scenes. It directly addresses the longstanding limitations of conventional techniques which often lack speed, flexibility, and point-of-care usability. The foundation of this system lies in a water-based, antibody-functionalized single-walled carbon nanotube (SWNT) bio-ink deposited onto chromatography paper, where wax-patterned barriers define microfluidic channels—significantly reducing fabrication cost and complexity while enabling scalable production and easy disposability.

The sensor's strong specificity and sensitivity, robust multiplexing potential, and ability to detect trace biomarker levels with minimal sample volume, even in aged, surface-deposited, or environmentally challenged samples, highlight its applicability at crime scenes, where biological evidence may be limited or compromised, and speedy analysis is critical. Additionally, the developed sensing strategy is highly adaptable and can be extended to detect a broad range of protein biomarkers, nucleic acids, and other biomolecules—making it a promising tool for rapid pathogen detection, and broader diagnostic use.

To enhance its practicality for field use, the sensor has been integrated with the Halibut smart tag, which enables wireless, real-time data transmission and eliminates the need for specialized laboratory equipment. With an estimated production cost of ~\$25 per unit, the Halibut system offers not only efficiency and portability but also economic scalability for widespread deployment. Beyond forensics, the software technologies developed through this work has potential applications in various domains that involve embedded systems, Internet-of-Things, and edge computing, spanning fields such as healthcare and environmental monitoring.

While originally designed for forensic applications, the versatility of this platform extends well beyond. In essence, this biosensor—smart tag system presents a versatile, affordable, and powerful solution for real-time analyte detection, especially in resource-limited forensic, clinical, and environmental settings where speed, accuracy, and accessibility are critical.

Limitations

 Minor variations in electrode patterning and drop-casting between channels may introduce inter-channel variability affecting signal consistency.

- Real biological samples from limited sources were used. Inter-individual differences in biomarker expression (e.g., due to health, hydration, diet) were not controlled.
- While the sensors demonstrated low limits of detection, their linear detection range remains limited due to antibody surface saturation, which restricts accurate measurement at very high analyte concentrations without prior dilution, especially for larger biomolecules.
- o In the algorithmic part, the proposed anomaly detection model (Hal-BG) showed reduced performance in certain scenarios, e.g., data after both sample placement and connection anomalies. This resulted in both false positives and false negatives that significantly affected recall and precision in those certain cases. Also, the method does not yet classify the type or source of detected anomalies. Further development is needed to automatically determine the specific nature of each anomaly and provide appropriate corrective actions.
- The implementation and validation were done for a fixed frequency (100Hz) for EIS measurements rather than the full spectrum scanning capabilities that would provide more comprehensive sensor characterization.
- Lastly, power optimization for battery operation has been designed but not fully characterized for field deployment scenarios with intermittent power availability.

Participants and Other Collaborating Organizations

Ashok Mulchandani - PI

Hyoseung Kim - Co-PI

Yu Shen - Graduate student (Research Assistant)

Touhid Bin Anwar - Graduate student (Research Assistant)

Samriddha Dutta - Graduate student (Research Assistant)

Ying Chen - Graduate student (Research Assistant)

Louay Fakhro - Graduate student (Research Assistant)

Abdulrahman Bukhari - Graduate student (Research Assistant)

Mohsen Karimi - Graduate student (Research Assistant)

Hyunjong Choi - Postdoc

Artifacts

Publications:

Journal Articles:

Manuscript: "Halibut: A Portable Device for Electrochemical Sensing with Anomaly Detection" (in preparation for journal submission)

- Y. Cheng, T. Pham and A. Mulchandani. "2D MoS2-based flexible electronic for biosensing," Sensors and Actuators B, 2025 (Accepted)
- A. Bukhari, S. Hosseinimotlagh and H. Kim. "OpenSense: An Open-World Sensing Framework for Incremental Learning and Dynamic Sensor Scheduling on Embedded Edge Devices," IEEE Internet of Things Journal, doi: 10.1109/JIOT.2024.3385016.
- Y. Shen and A. Mulchandani. "Affordable paper-based SWNTs field-effect transistor biosensors for nucleic acid amplification-free and label-free detection of micro RNAs," Biosensors and Bioelectronics:X, 100364, 2023.
- Y. Shen, T. B. Anwar and A. Mulchandani. "Current status, advances, challenges and perspectives on biosensors for COVID-19 diagnosis in resource-limited settings," Sensors and Actuators Reports, 3, 100025, 2021.
- M. Sedki, Y. Shen and A. Mulchandani. "Nano-FET-enabled biosensors: Materials perspective and recent advances in North America," Biosensors and Bioelectronics, 176, 112941, 2021.
- Y. Shen, S. Modha, H. Tsutsui and A. Mulchandani. "An origami electrical biosensor for multiplexed analyte detection in body fluids," Biosensors and Bioelectronics, 171, 112721, 2021.
- H. S. Magar, R. Y. A. Hassan and A. Mulchandani. "Electrochemical Impedance Spectroscopy (EIS): Principles, Construction, and Biosensing Applications," Sensors, 21, 6578, 2021.

Conference Abstracts:

- S. Dutta, Y. Shen and A. Mulchandani. Poster: "Nanobiosensor Arrays for Rapid On-Site Multiplexed Detection of Forensically Relevant Body Fluids at Crime Scenes," 2025 NIJ Forensic Science R&D Symposium, Pittcon, March 3, 2025, Boston, MA.
- S. Dutta, Y. Shen and A. Mulchandani. Oral: "Nanobiosensor Arrays for Rapid On-Site Multiplexed Detection of Forensically Relevant Body Fluids at Crime Scenes," 2025 NIJ Forensic Science R&D Symposium, Pittcon, March 4, 2025, Boston, MA.
- S. Dutta, Y. Shen and A. Mulchandani. Poster: "Nanobiosensor arrays for rapid on-site multiplexed detection of forensically relevant body fluids at crime scenes," Pittcon, 27 February, 2024, San Diego, CA.

- A. Bukhari and H. Kim. Poster: "Learning-based Sensor Scheduling for Event Classification on Embedded Edge Devices," In ACM/IEEE International Conference on Internet of Things Design and Implementation (IoTDI), 2023.
- A. Mulchandani. Oral: "Towards ASSURED diagnostics using paper-microfluidic integrated chemiresistor biosensor arrays", International Conference on Bioinformatics and Biomedical Engineering, July 12-14, 2023, Gran Canaria, Spain.
- S. Dutta, Y. Shen and A. Mulchandani. Poster: "Paper-based chemiresistive biosensor arrays for rapid, on-site identification of multiple body fluids at a crime scene," 2023 NIJ Forensic Science R&D Symposium, Orlando, FL, February 14, 2023.
- M. Karimi, Y. Wang and H. Kim. Oral: "Energy-Adaptive Real-time Sensing for Batteryless Devices," In IEEE International Conference on Embedded and Real-Time Computing Systems and Applications (RTCSA), 2022.
- A. Bukhari, S. Hosseinimotlagh and H. Kim. Oral: "An Open-World Time-Series Sensing Framework for Embedded Edge Devices," In IEEE International Conference on Embedded and Real-Time Computing Systems and Applications (RTCSA), 2022.
- T. B. Anwar, Y. Shen and A. Mulchandani. Oral: "Paper microfluidic single-walled carbon nanotubes chemiresistive biosensor arrays for body fluids identification," 2021 NIJ R&D Symposium/ American Academy of Forensic Sciences 73rd Annual Meeting, Feb 15, 2021, Virtual.
- T. B. Anwar, Y. Shen and A. Mulchandani. Oral: "Biosensor arrays for multiplexed identification of body fluids," Pittcon 2021, March 11, 2021, Virtual.
- Y. Shen and A. Mulchandani. Oral: "Paper-based field-effect transistor biosensor for affordable point-of-care detection of microRNAs at sub-attomolar level for potential cancer diagnosis," 262nd ACS National Meeting and Exposition, August 25, 2021.

Software and Hardware Artifacts

"Halibut" portable electrochemical sensing platform hardware design files

Halibut firmware (C/C++ for microcontroller operation)

GUI application (Python/Kivy for cross-platform interface)

Hal-BG anomaly detection model implementation

Data Sets Generated

Labeled measurement dataset of normal sensor behavior and anomalies

Dissemination Activities

Conference Presentations:

- S. Dutta, Y. Shen and A. Mulchandani. Poster: "Nanobiosensor Arrays for Rapid On-Site Multiplexed Detection of Forensically Relevant Body Fluids at Crime Scenes", 2025 NIJ Forensic Science R&D Symposium, Pittcon, March 3, 2025, Boston, MA.
- S. Dutta, Y. Shen and A. Mulchandani. Oral: "Nanobiosensor Arrays for Rapid On-Site Multiplexed Detection of Forensically Relevant Body Fluids at Crime Scenes", 2025 NIJ Forensic Science R&D Symposium, Pittcon, March 4, 2025, Boston, MA.
- S. Dutta, Y. Shen and A. Mulchandani. Poster: "Nanobiosensor arrays for rapid on-site multiplexed detection of forensically relevant body fluids at crime scenes," 2024 NIJ Forensic Science R&D Symposium, Pittcon, San Diego, CA, February, 27, 2024.
- S. Dutta, Y. Shen and A. Mulchandani. Poster: "Paper-based chemiresistive biosensor arrays for rapid, on-site identification of multiple body fluids at a crime scene," 2023 NIJ Forensic Science R&D Symposium, Orlando, FL, February 14, 2023. https://forensiccoe.org/private/63f50fb8781f2

Samriddha Dutta, Yu Shen and Ashok Mulchandani. Webinar: "Advanced Forensic Methods: Identifying Body Fluids at Crime Scenes", 2023 NIJ Forensic Science R&D Webinar Series, November 9, 2023. https://forensiccoe.org/webinar-2023-nijrd-fluid-identification/

- A. Bukhari and H. Kim. Poster: "Learning-based Sensor Scheduling for Event Classification on Embedded Edge Devices," In ACM/IEEE International Conference on Internet of Things Design and Implementation (IoTDI), 2023.
- M. Karimi, Y. Wang and H. Kim. Oral: "Energy-Adaptive Real-time Sensing for Batteryless Devices," In IEEE International Conference on Embedded and Real-Time Computing Systems and Applications (RTCSA), 2022.
- A. Bukhari, S. Hosseinimotlagh and H. Kim. Oral: "An Open-World Time-Series Sensing Framework for Embedded Edge Devices," In IEEE International Conference on Embedded and Real-Time Computing Systems and Applications (RTCSA), 2022.
- T. B. Anwar, Y. Shen and A. Mulchandani. Oral: "Paper microfluidic single-walled carbon nanotubes chemiresistive biosensor arrays for body fluids identification" 2021 NIJ R&D Symposium/American Academy of Forensic Sciences 73rd Annual Meeting, Feb 15, 2021, Virtual.
- T. B. Anwar, Y. Shen and A. Mulchandani. Oral: "Biosensor arrays for multiplexed identification of body fluids," Pittcon 2021, March 11, 2021, Virtual.